PROCEEDINGS OF SCIENCE

Searching for Primordial Black Hole as Dark matter by cross-correlation with MeV γ-ray emissions

Xiu-hui Tan,[a,*] **Jun-qing Xia,**[a] **Yang-jie Yan**[a] **and Taotao Qiu**[b]

[a] *Beijing Normal University,Department of Astronomy, 19 Xinwai Street, Beijing, People's Republic of China*

[b] *Huazhong University of Science and Technology, School of Physics, 1037 Luoyu Road, Wuhan, People's Republic of China*

E-mail: tanxh@bnu.edu.cn

Primordial black holes (PBHs) as potential candidates for dark matter have recently regained wide attention. We focus on the Hawking radiation of PBHs, utilizing the cross-correlation between MeV γ-ray emissions and the lensing effect of the cosmic microwave background (CMB). Near-future data can provide tight constraints on the fraction of Schwarzschild PBHs with masses around 10^{17} g, we consider the CMB-S4 project and the γ-ray telescope e-ASTROGAM for this purpose. Additionally, we consider the conservative astrophysical model as a reference for the observed emissions in the MeV energy range. Moreover, we can enhance our constraining capability by an order of magnitude when taking the PBHs model with spins into account. This technology, coupled with appropriate data, bears significance in bridging the gaps in determining PBHs fraction limits within the asteroid mass range.

38th International Cosmic Ray Conference (ICRC2023)
26 July - 3 August, 2023
Nagoya, Japan

*Speaker

PoS(ICRC2023)1364

1. Introduction

The primordial black holes (PBHs) as dark matter (DM) candidates stems have reemphasized recently. This is not only due to the groundbreaking detection of the first binary black holes merger by the LIGO-Virgo collaboration [1], but also from the fact that they do not require exotic particles beyond the Standard Model [2]. PBHs are formed during the early stages of the cosmic radiation-dominated era through various mechanisms. Under the theoretical hypothesis, various constraints for PBHs have proposed, by the signal from gravitational-lensing, dynamical effects, accretion, gravitational waves and Hawking Evaporation (HE) [3, 4]. However, PBHs weighing less than 5×10^{14}g can not survive util today [5]. A wealth of observational data is available to strongly constrain a crucial parameter of PBHs, namely the fraction $f_{\rm PBH} \equiv \Omega_{\rm PBH}/\Omega_{\rm DM}$. PBHs within the asteroid mass range ($1 \times 10^{16} - 10^{23}$g) still possess significant uncertainty regarding their fraction, leaving ample room for further exploration.

Several recent studies have focused on the upcoming AMEGO and e-ASTROGAM projects. This work is based on [6], we consider PBHs as a type of DM formed through gravitational interaction, utilize the γ-ray emissions of a specific energy range from the HE, to track the spatial distribution of PBHs within the large-scale structure of the Universe. Additionally, there exists an inherent connection between the CMB, which forms from the primordial perturbation as well. Therefore, we can infer a relationship between the γ-ray emissions from PBHs and the CMB lensing signal. To explore this relationship, we employ cross-correlation technique, which is extensively used and sophisticated for indirect detection of DM in previous studies [7, 8], to search this kind of connection by simulating the future e-ASTROGAM and CMB-S4 [9] projects and constrain the PBHs fraction.

2. Models

The γ-ray emissions in the MeV range produced by PBHs could trace the density field. Therefore, the source field of PBHs provides a primordial seed for the specific observable along the line of sight direction. In order to implement cross-correlation, we first define the window function of PBHs:

$$W_{\rm PBH}(\chi) = \frac{f_{\rm PBH}\Omega_{\rm DM}\rho_c}{4\pi M_{\rm PBH}} \times \int_{\delta E}\int_{t_{\rm min}}^{t_{\rm max}} \left[\frac{{\rm d}^2 N}{{\rm d}t{\rm d}E_\gamma}\right]_{\rm tot} E_\gamma(\chi) e^{-\tau[\chi, E_\gamma(\chi)]} {\rm d}E_\gamma {\rm d}t \ , \tag{1}$$

where ${\rm d}^2N/{\rm d}t{\rm d}E_\gamma$ denotes the number of particles N emitted per units of energy and time, both primary and secondary spectra are considered, with the latter being generated from processes such as decay or hadronization of primary particles. $\chi = \chi(z)$ represents the comoving distance, and $\tau[\chi, E_\gamma(\chi)]$ is the optical depth. The time integral runs from $t_{\rm min} = 380,000$ years at last scattering of the CMB to $t_{\rm max} = \min(t(M), t_0)$ where $t(M)$ is the PBHs lifetime with mass M and t_0 is the age of the Universe.

PBHs formed during radiation time tend to have low spin with $a_* \lesssim 0.4$ according to a theoretical prediction from [10], but we give a mild $a_* = 0.5$ and an extreme spin $a_* = 0.9999$ for

comparison with the $a_* = 0$ case. In our calculations, we use the public software `BlackHwak` [11] to generate the photon spectra with three spin conditions, $a_* = \{0, 0.5, 0.9999\}$.

The CMB lensing convergence, κ, in a given line of sight is the integral over all the matter fluctuations that will cause gravitational lensing, $\kappa(\hat{\mathbf{n}}) = \int dz W_\kappa(z)\delta(\chi\hat{\mathbf{n}}, z)$, where $\delta(\chi\hat{\mathbf{n}}, z)$ is the overdensity of matter at comoving distance χ and redshift z. The distance kernel, $W_\kappa(z)$, is given by

$$W_\kappa(z) = \frac{3}{2}\Omega_{\rm m}H_0^2\frac{1+z}{H(z)}\frac{\chi(z)}{c}\left[\frac{\chi_{\rm cmb}-\chi(z)}{\chi_{\rm cmb}}\right], \tag{2}$$

where $\Omega_{\rm m}$ is the fraction of the matter density today compared to the present critical density of the Universe, H_0 is the Hubble parameter today, $H(z)$ is the Hubble parameter as a function of redshift, c is the speed of light and $\chi_{\rm cmb}$ is the comoving distance to the surface of last scattering where the CMB was emitted.

Besides the PBHs emission by the HE, the clusters of galaxies, AGNs and galaxies can also provide the significant contributions to the MeV γ-ray emission of the sky. Among these three astrophysical sources, the clusters of galaxies can emit high energy emissions by means of bremsstrahlung radiation of their gas. We calculated the intensity from bremsstrahlung radiation according to Ref. [12] and find that the main contribution of the clusters appears in the energy band < 40 keV, which is not covered by the energy range of the e-ASTROGAM project. Therefore, in the following calculations, we neglect the contribution from the clusters. The window functions $W(z)$ of AGNs and galaxies are given by:

$$W_{\rm X}(E,z) = \int_{L_{\rm X,min}}^{L_{\rm X,max}(F_{\rm sens},z)}\frac{{\rm d}L_{\rm X}}{L_{\rm X}}\Phi_{\rm X}(L_{\rm X},z)\mathcal{L}_{\rm X}(E,z), \tag{3}$$

where $\Phi_{\rm X}$ is the luminosity function, $\Phi_{\rm X}(E,z)$ denotes the differential luminosity at an energy E (defined as a number of photon emitted per unit time and per unit energy range) at redshift z. We set the minimal luminosity $L_{\rm X,min} = 10^{39}\,{\rm erg\,s^{-1}}$, while the maximum luminosity $L_{\rm X,max}$ of an unresolved source is dictated by the sensitivity flux $F_{\rm sens}$ of the γ-ray experiment, providing the minimum detectable flux. The intensity provided by the astrophysical emitters is reported in Fig.1, where we compare the prediction of intensity from PBHs.

As the γ-ray emissions intensity from PBHs is expected to be biased tracers of matter fluctuations, the cross-correlation power spectrum between γ-ray emissions intensity from PBHs and CMB lensing is:

$$C_\ell^{\kappa,{\rm PBH}} = \int\frac{{\rm d}z}{c}\frac{H(z)}{\chi^2(z)}W_\kappa(z)W_{\rm PBH}(z)P_{\kappa,{\rm PBH}}(k=\ell/\chi,z), \tag{4}$$

where $P_{\kappa,{\rm PBH}}$ is the 3D power spectrum of cross-correlation between CMB lensing and the γ-ray emissions from PBHs, which consists of two parts in the halo model, $P_{\kappa,{\rm PBH}} = P^{\rm 1h}_{\kappa,{\rm PBH}} + P^{\rm 2h}_{\kappa,{\rm PBH}}$, and the mass integral runs from $M_{\rm min} = 10^7 M_\odot$ to $M_{\rm max} = 10^{18}M_\odot$. For the halo bias of PBHs, we directly take from the equation (12) of [13]. Furthermore, we include the contribution from the iso-curvature perturbation to the linear part, as well as the halo mass function of PBHs are calculated, following as [14]. Similar with Eq.(4), we can also obtain the cross-correlation signals between the CMB lensing and two astrophysical sources, which are shown in Fig.2.

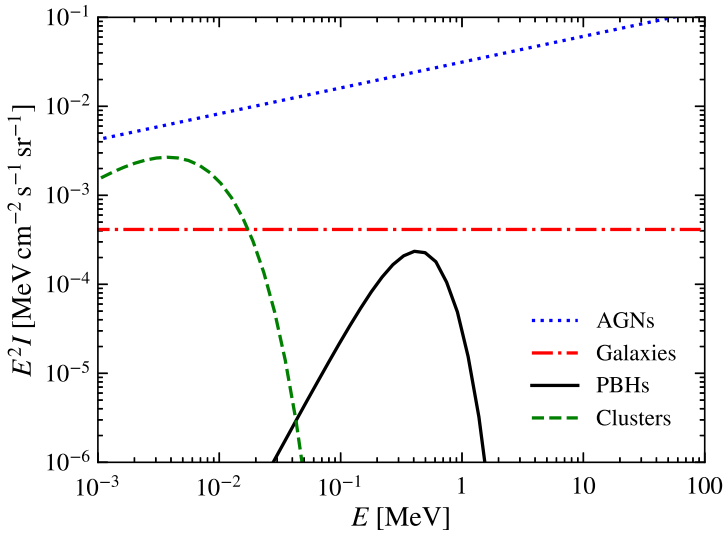

Figure 1: Total intensity produced by AGN (blue dotted line), galaxies (red dash-dotted line), and the cluster of galaxies (green dashed line). For comparison, we also plot the PBHs emission (black solid line) with $M_{\rm PBH} = 10^{17}$ g, the spin $a_* = 0$ and the fraction $f_{\rm PBH} = 10^{-3}$.

The power spectrum of AGNs contributes most of the signal, while the signal from galaxies is much smaller and mainly on large scales. Here, we also illustrate the signals from PBHs with different fraction values to demonstrate their effects on the cross-correlation power spectrum signal. From the black curves in the figure, we can see the signal from PBHS will be comparable to that from AGN when $f_{\rm PBH} = 10^{-3}$.

3. Future Experiments

In this study, we assess the potential of an instrument possessing the sensitivity of e-ASTROGAM to examine the constraining capabilities on the fraction of Primordial Black Holes (PBHs). The e-ASTROGAM observatory is dedicated to the investigation of the non-thermal Universe within the photon range of 0.15 MeV to 3 GeV by a γ-ray telescope [15]. We adapted the effective area, angular resolution, and flux sensitivity, exhibit variations across different energy intervals as specified in Table III and IV of [16]. Employing an observational time of 10^6 seconds, we focus our examination on a sky fraction of $f_{\rm sky} = 0.23$, corresponding to a field of view of $\Omega = 2.9$ steradians. The flux sensitivity of 1.1×10^{-12}erg, cm^{-1}, s^{-1} is adopted uniformly throughout the entire energy range, while the particle background registers a count rate of 1.4 counts s^{-1}, sr^{-1}.

It is evident that higher mass PBHs generate photon emissions at lower energy levels, so for PBH masses $M_{\rm PBH} > 5 \times 10^{17}$, g, the peak energy $E_{\rm peak}$ exceeds the energy range capability of e-ASTROGAM. Consequently, we have excluded photons near the peak energy (refer to Tab. 1) and solely considered lowest photons within the energy range of e-ASTROGAM, i.e., from 150 keV to 300 keV, during the calculations.

In order to conduct CMB lensing studies, we adopt a CMB-S4 experiment [9], which features a telescope beam with a Full-Width-Half-Maximum (FWHM) of 1′, with temperature and polarization

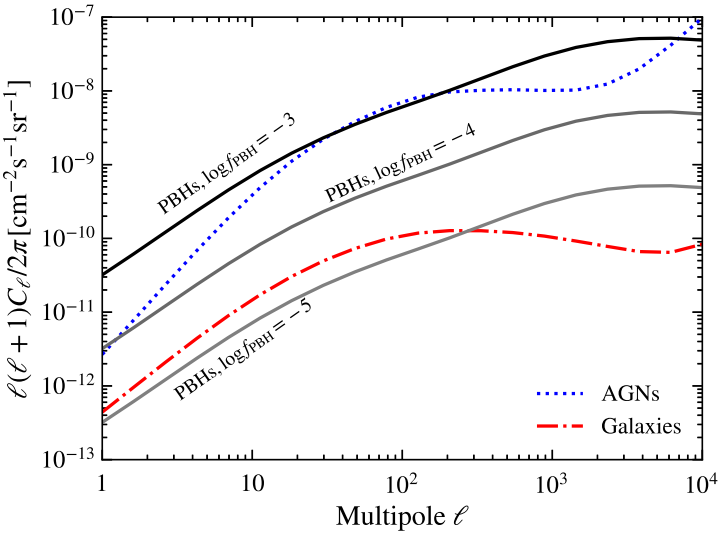

Figure 2: Cross-correlation angular power spectra between the CMB lensing and AGNs (blue dotted line), galaxies (red dash-dotted line), and PBHs (black solid lines). Here, we choose the PBHs mass $M_{\mathrm{PBH}} = 10^{17}$ g, the spin $a_* = 0$. From top to bottom, we show power spectra from different values of the PBHs fraction: $f_{\mathrm{PBH}} = 10^{-3}$, 10^{-4}, 10^{-5}, respectively.

Table 1: The best energy performance E_{peak} (keV) used for different masses of PBHs, according to e-ASTROGAM.

M_{PBH} (g)	1×10^{16}	3×10^{16}	5×10^{16}	7×10^{16}	1×10^{17}	3×10^{17}	5×10^{17}	7×10^{17}	1×10^{18}	3×10^{18}	5×10^{18}
$a_* = 0$	4690	2234	1204	831	448	213	150	102	50	23	12
$a_* = 0.5$	4690	2234	1362	940	507	213	150	102	50	23	12
$a_* = 0.9999$	7690	3662	2234	1541	831	350	213	167	79	38	20

white noise levels of 1 $\mu K'$ and 1.4 $\mu K'$, respectively. Our approach involves setting the primary CMB noise levels N_ℓ^{TT} and N_ℓ^{EE} as Gaussian noise distributions: $N_\ell^{\mathrm{XX}} = s^2 \exp\left(\ell(\ell+1)\frac{\theta^2_{\mathrm{FWHM}}}{8\log 2}\right)$, where XX stands for TT or EE, s is the total intensity of instrumental noise in μK rad, and θ^2_{FWHM} is the FWHM of the beam in radians. For the CMB lensing reconstruction noise, we use the EB quadratic estimator method described in [17], implemented by the `QUICKLENS` software package [1].

Finally, We choose the proper energy range for integration for each mass of PBHs, which is around the E_{peak} listed in the Tab.1. The redshift range we consider is from 0 to 10. Furthermore, we assume the flat ΛCDM cosmology with parameters set by *Planck* results [18]: $h = 0.6766$, $\Omega_{\mathrm{b}}h^2 = 0.02243$, $\Omega_{\mathrm{c}}h^2 = 0.11999$, $\tau = 0.0561$, and $n_s = 0.9665$.

[1] https://github.com/dhanson/quicklens/

4. Results

Assuming the experiments are the power spectra of Gaussian random fields, we can compute the covariance matrix as the following:

$$\Gamma^{\gamma,\kappa}_{\ell,\ell'} = \frac{\delta_{\ell\ell'}}{(2\ell+1)\, f_{\rm sky}\Delta\ell} \times \left[C^{\gamma\kappa}_{\ell} C^{\gamma\kappa}_{\ell'} + \left(C^{\gamma}_{N} + \sqrt{C^{\gamma}_{\ell} C^{\gamma}_{\ell'}} \right) \left(C^{\kappa}_{N} + C^{\kappa}_{\ell} \right) \right], \tag{5}$$

where the photon noise term above is $C^{\gamma}_{N} = 4\pi f_{\rm sky} \langle I_{\rm X} \rangle^2 N_{\rm X}^{-1} W_{\ell}^{-2}$, and $\langle I_{\rm X} \rangle$ refers to the sky-averaged intensity observed by the telescope, and is assumed that comes from the AGNs and galaxies contributions by default; $N_{\rm X} = \langle I_{\rm X} A_{\rm eff} \rangle\, t_{\rm obs} \Omega_{\rm FoV}$; the beam window $W_{\ell} = \exp\left(-\sigma_{\rm b}^2 \ell^2/2\right)$ is a Gaussian point-spread function.

The upper limits on the parameter space of the PBHs fraction are derived at 95% confidence level by requiring $\chi^2 = 2.71$ with the estimator assumed to follow a χ^2 distribution with one degree of freedom defined as, $\chi^2 = \sum_{\ell} \left(C^{\gamma,\kappa}_{\ell} \Gamma^{-1}_{\ell\ell'} C^{\gamma,\kappa}_{\ell'} \right)$, where the sum of multipoles is from $\ell_{\rm min} = 10$ to $\ell_{\rm max} = 10^3$, respecting the beam window function of e-ASTROGAM. It is important to highlight that in the signal part of the χ^2 function, only the cross-correlation term involving the PBHs is considered. This assumption is made under the premise that we are capable of accurately extracting the background associated with the emitting AGNs and galaxies, while disregarding model uncertainties in the astrophysical components. Additionally, we avoid summing up the energy bins due to the fact that for every PBH mass, the integration energy range will vary around the different $E_{\rm peak}$ values mentioned earlier.

In Figure 3, we present the 95% confidence level (C.L.) forecasted constraint bound on the fraction of primordial black holes (PBHs) for different PBH masses. The solid blue line represents our main result for standard Schwarzschild PBHs. The cross-correlation between γ-ray emissions and CMB lensing significantly narrows down the allowed range of $f_{\rm PBH}$ for low mass PBHs. The tight constraint can be obtained from e-ASTROGAM is primarily due to its high sensitivity to flux, which is a crucial factor in the measurement of photon noise. The high sky-averaged intensity ($\langle I_{\rm X} \rangle$) observed by the telescope leads to a suppression of the shot noise term in the covariance matrix (Eq.(5)) and improves the precision of the constraints on the PBHs fraction ($f_{\rm PBH}$).

5. Conclusions

In this work, we analyze the cross-correlation signal within the redshift range of $0-10$ (z-all), which forecast highly precise constraints on the fraction of PBHs with masses ranging from 10^{16} to 10^{18} g. To further explore the effectiveness of constraint on the PBHs fraction, we modify the integration range by considering two additional redshift ranges: $0-1$ (z-low) and $1-10$ (z-high). Fig.3 shows the results on $f_{\rm PBH}$ for the z-low (green solid line) and z-high (red solid line) cases. While z-low case is very close to the z-all case, which indicates that the effect from astrophysical sources is mainly from the low-redshift Universe. In addition, Figure 3 presents three different spins: $a_* = 0.5$ (blue dashed line) and $a_* = 0.9999$ (blue dotted line). $f_{\rm PBH}$ is greatly enhanced by more than an order of magnitude when PBHs are extremely rotational. The emission from active galactic nuclei (AGNs) still dominates even at lower energy bands. Therefore, regardless of whether

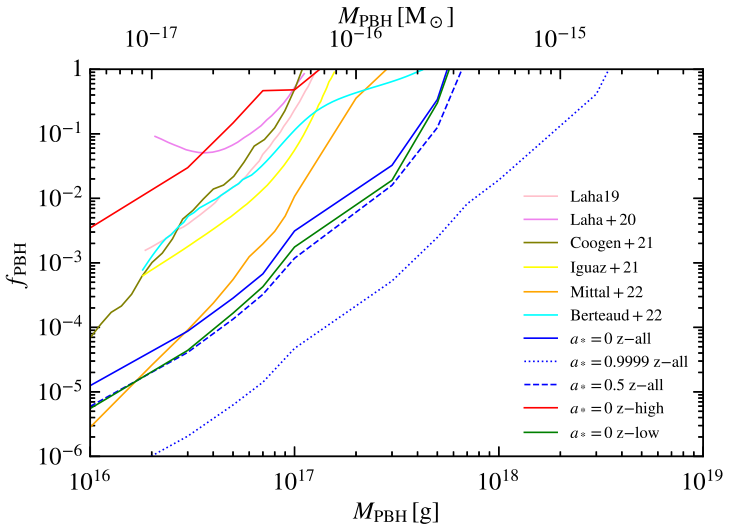

Figure 3: 95% C.L. bounds on the PBHs fraction as a function of the PBHs masses, when considering different cases. We plot some important PBHs works for comparison, the Galactic Center 511 keV line [19] (the pink line); from published SPectrometer aboard the INTEGRAL satellite (SPI) results [20] (the purple line); using cosmic X-ray background [21] (the yellow line) and from diffuse soft γ-ray emission towards the inner Galaxy as measured by the SPI data [22] (the cray line), Comptel observations of the central region of the Galaxy (the olive line) [23], and as well as the recent limitation (the orange line) from the 21-cm absorption signal of EDGES experiment at $M_{\rm PBH} > 10^{17}$ g [24].

the cluster of galaxies is included in the calculations or not, the final constraints should not undergo significant changes.

By leveraging future projects such as e-ASTROGAM and CMB-S4, we are able to establish highly stringent limitations on the Schwarzschild PBHs fraction within the mass range of 10^{16} – 5×10^{17} g. We are interested in other particles generated by HE from PBHs and other radiation processes during propagation, which is promisingly addressing the gaps in the limits of PBHs fraction within the asteroid mass range.

References

[1] LIGO Scientific and Virgo Collaborations, B.P. Abbott et al. 2016, Physical Review Letter, 116, no.6, 061102

[2] B. Carr, F. Kuhnel and M. Sandstad, 2016 Physical Review D, 94, no.8, 083504

[3] B. Carr and F. Kuhnel, SciPost Phys. Lect. Notes **48**, 1 (2022)

[4] S. W. Hawking, 1975 Commun. Math. Phys. 43, 199

[5] J. H. MacGibbon, B. J. Carr and D. N. Page, 2008, Phys. Rev. D, 78, 064043

[6] X. H. Tan, Y. J. Yan, T. Qiu and J. Q. Xia, Astrophys. J. Lett. **939**, no.1, L15 (2022)

[7] A. Cuoco, J. Q. Xia, M. Regis, E. Branchini, N. Fornengo and M. Viel, 2015, Astrophys. J. Suppl., 221, no.2, 29

[8] X. Tan, M. Colavincenzo and S. Ammazzalorso, 2020, Mon. Not. Roy. Astron. Soc., 495, no.1, 114-122

[9] CMB-S4 Collaboration, K. N. Abazajian, et al.

[10] T. Chiba and S. Yokoyama, 2017, PTEP, 2017, no.8, 083E01

[11] A. Arbey and J. Auffinger, 2021, Eur. Phys. J. C, 81, 10

[12] F. Zandanel, C. Weniger and S. Ando, 2015, JCAP, 09, 060

[13] R. K. Sheth and G. Tormen, 1999, Mon. Not. Roy. Astron. Soc., 308 119

[14] J. O. Gong and N. Kitajima, 2017, JCAP, 08, 017

[15] e-ASTROGAM, V. Tatischeff et al., 2018 Proc. SPIE Int. Soc. Opt. Eng., 10699, 106992J

[16] e-ASTROGAM, A. De Angelis et al., 2017 Exper. Astron., 44, no.1, 25-82

[17] W. Hu and T. Okamoto, 2002, Astrophys. J., 574, 566-574

[18] N. Aghanim et al., 2020 Astronomy & Astrophysics, 641, A6

[19] R. Laha, 2019, Phys. Rev. Lett., 2019, 123 no.25, 251101

[20] R. Laha, J. B. Muñoz and T. R. Slatyer, 2020, Phys. Rev. D, 101, no.12, 123514

[21] J. Iguaz, P. D. Serpico and T. Siegert, 2021, Phys. Rev. D, 103, no.10, 103025

[22] J. Berteaud, F. Calore, J. Iguaz, P. D. Serpico and T. Siegert, 2022, Phys. Rev. D, 106, no.2, 023030

[23] A. Coogan, L. Morrison and S. Profumo, 2021, Phys. Rev. Lett., 126, no.17, 171101

[24] S. Mittal, A. Ray, G. Kulkarni and B. Dasgupta, 2022 JCAP, 03, 030